# Excitation-multiplexed multicolor super-resolution imaging with fm-DNA-PAINT and fm-STORM

Pablo A. Gómez-García[1,2], Erik T. Garbacik[1], Jason J. Otterstrom[1,&] Maria F. Garcia-Parajo[1, 3, #,*], Melike Lakadamyali[1, 4, #, *]

[1]ICFO-Institut de Ciencies Fotoniques, The Barcelona Institute of Science and Technology, 08860 Castelldefels (Barcelona), Spain.

[2]Centre for Genomic Regulation (CRG), The Barcelona Institute of Science and Technology, Spain

[3]ICREA, Pg. Lluís Companys 23, 08010 Barcelona, Spain.

[4]Perelman School of Medicine, Department of Physiology, University of Pennsylvania, Clinical Research Building, 415 Curie Blvd, Philadelphia, PA, 19104

[&] Current address: IDEA Bio-Medical, Parc Mediterrani de la Tecnologia, RDIT building, 08860 Castelldefels (Barcelona), Spain.

* Correspondence should be addressed to ML: melikel@pennmedicine.upenn.edu and MFG-P: maria.garcia-parajo@icfo.eu

# These authors contributed equally to this work



www.pnas.org/cgi/doi/10.1073/pnas.1804725115

## SI Methods:

### Sample preparation for fm-DNA-PAINT and fm-STORM:

BSC1 cells were cultured at 37ºC with 5% $CO_2$. Cell culture consisted of complete growth medium (Minimum Essential Medium Eagle with Earle's salts and nonessential amino acids plus 10% (v/v) FBS, 2 mM L-glumine, and 1 mM sodium pyruvate). For the imaging experiments, cells were plated on 8-well Lab-Tek 1 coverglass chamber (Nunc) at a seeding density of 20000–50000 cells per well. After 24 hours of incubation, cells were fixed with fixation buffer consisting of 3% paraformaldehyde and 0.1% of glutaraldehyde in PBS at 37ºC during 10 minutes. The background fluorescence of glutaraldehyde was quenched by 0.1% of $NaBH_4$ solution in PBS during 7 minutes at room temperature. After fixation, blocking buffer solution was applied (3% (w/v) BSA, 0.2% TritonX-100 (Fisher Scientific) (v/v) in PBS) for 60 minutes.

For immunofluorescence, cells were labeled with the appropriate primary and secondary antibodies. For fm-DNA-PAINT, rabbit-anti-alpha-tubulin primary antibody (ab18251 Polyclonal, AbCam) at a dilution of 1:150 and mouse-anti-TOM20 primary antibody (WH0009804M1 Monoclonal, Sigma Aldrich) at a dilution of 1:150 in blocking buffer were used to label microtubules and mitochondria, respectively. For secondary antibodies, oligo-functionalized goat- anti-mouse (1:100 dilution in blocking buffer) and goat-anti-rabbit (1:100 dilution in blocking buffer) secondary antibodies included in the Ultivue-2 kit (Ultivue, Inc) were used. For fm- STORM, rabbit-anti-TOM20 (sc-11415, Santa Cruz Biotechnologies) and rat-anti-alpha-tubulin (MAB1864-I, Clone YL1/2, Merck), primary antibodies were used at a dilution of 1:150 and 1:150 in blocking buffer to label mitochondria and microtubules, respectively. Donkey-anti-rabbit conjugated with Cy3b/AF405 and donkey-anti-rat conjugated with AF647/AF405 were used as secondary antibodies. The secondary antibodies were custom labeled with the fluorophore pairs as previously described (1). The training dataset for the cross-talk correction algorithm implemented for fm-STORM was prepared and imaged in the exact same way with the exception that only one primary and appropriate secondary antibody was used to label a single structure. fm-DNA-PAINT was performed in an imaging buffer with high ionic phosphate strength provided in Ultivue-2 kit. fm-STORM was performed in an imaging buffer containing GLOX solution as oxygen scavenging system (40 $mg/mL^{-1}$ Catalase [Sigma], 0.5 $mg/ml^{-1}$ glucose oxidase, 10% Glucose in PBS) and MEA 10 mM (Cysteamine MEA [SigmaAldrich, #30070-50G] in 360mM Tris-HCl).

### Optical setup:

Imaging was performed on a custom-built inverted Nikon Eclipse Ti microscope (Nikon Instruments). The excitation module is equipped with four excitation laser lines: 405 nm (100 mW, OBIS Coherent, CA), 488 nm (200 mW, Coherent Sapphire, CA), 561 nm (500 mW MPB Communications, Canada) and 647 nm (500 mW MPB Communications, Canada). The laser beams intensities were sinewave modulated through AOMs (AA Opto Electronics MT80 A1,5Vis) at different frequencies ranging from 50 Hz to 10 Hz, depending on the modality and

on the imaging conditions. The different wavelengths were combined and coupled into the microscope objective through dichroic mirrors. The same objective (Nikon, CFI Apo TIRF 100x, NA 1.49, Oil) was used for illumination and for collecting the fluorescence signal. The focus was locked through the Perfect Focus System (PFS, Nikon). Fluorescence emitted signal then passed through a notch filter "Quad Band" (ZT405/488/561/647rpc-UF2, Chroma Technology) that blocks just the excitation laser lines. Imaging was performed on an EM-CCD camera (Andor iXon X3 DU-897, Andor Technologies). The pixel size after the 100X magnification was 160 nm.

We note that chromatic aberrations affect all super-resolution multicolor approaches that use spectrally different reporter dyes, including the frequency multiplexed imaging implementation reported here. Chromatic aberrations lead to a shift in the center position of the localizations between different channels that is on the range of tens of nanometers (~ 10-40 nm), depending on the wavelengths and the imaging conditions (2). Fiducial markers like beads can be used to correct for this offset, and typically yield alignment precisions below or comparable to the localization precision (2).

**fm-DNA-PAINT imaging conditions:**

Imaging for fm-DNA-PAINT modality was performed using highly inclined (HiLo) illumination (3) with an excitation intensity of ~300W/cm$^2$ for the 561nm and 647nm laser lines. Camera frame rate of 60 Hz was used for the experiments with a field of view of 128x128 pixels (20 μm x 20 μm). The 647 nm and 561 nm lasers were modulated with sinusoidal waves at 30 Hz and 20 Hz, respectively. For 3D imaging, a cylindrical lens was used to encode the *z* position of the molecules into the PSF shape (4).

**fm-STORM imaging conditions:**

Imaging for fm-STORM modality was performed using HiLo illumination (3) with an excitation intensity of ~1.8kW/cm$^2$ for the 561nm and the 647nm laser lines, and ~1kW/cm$^2$ for the 488nm laser line. The 405nm laser line was used in continuous illumination mode for the reactivation of the fluorophore pairs. The 405nm laser intensity follows a ramp (ranging from ~10W/cm$^2$ to ~25W/cm$^2$), in order to maintain a relatively constant density of fluorophores per frame. Camera frame rate of 90 Hz was used for the experiments with a field of view of 128x128 pixels (20 μm x 20 μm). 647 nm and 561 nm lasers were modulated with a sinewave at 45 Hz and 22.5 Hz. For the 3-color data sets, the 647nm, 561nm and 488nm lasers were modulated at 45 Hz, 30 Hz and 15Hz, respectively.

**fm-DNA-PAINT data analysis:**

Demodulation of the raw data was carried out using a custom written Python code (deposited on GitHub: https://github.com/PabloAu/Excitation-multiplexed-multicolor-super-resolution-imaging-with-fm-DNA-PAINT-and-fm-STORM). For the demodulation, packages of 6 frames (frame window size, *m*) were used in order to maintain the long effective exposure time required for DNA-Paint (we chose 100 ms). The intensity evolution of each pixel from

these 6 frames was transformed to the frequency domain using a one-dimensional Discrete Fourier Transform for real input:

$$X_k = \sum_{n=0}^{m-1} x_n \cdot e^{-i2\pi k \cdot \frac{n}{m}};\ k = 0, \ldots, m-1$$

where, $X_0,\ldots,X_{m-1}$ are the Fourier Transformed output values in the discrete frequency domain, $x_0,\ldots,x_{m-1}$ are the real discrete input values from time domain, and *m* is the total number of real input values (equal to the frame window size).

The Discrete Fourier Transform presents symmetry. $X_0$ and $X_{m/2}$ are real values. The rest of the output values from the DFT are specified by (m/2)-1 complex numbers, because the remaining output values are the conjugated ones. Therefore, a 6 frame window size (*m* = 6), will provide 3 frequency bins and thus 3 available channels (see **Fig. 2a** of the main text). The $X_0$ corresponds to DC component and contains no valuable information, while the AC components encode the amplitudes at which the fluorophore absorbs each excitation laser, and hence reveal the spectral characteristics of that localization.

For this calculation, we used the efficient Fast Fourier Transform algorithm (FFT). The absolute values of the amplitudes in the frequency domain were used to assign a pixel value to its channel on the demodulated data, corresponding to each frequency bin in use. With a frame window of 6 frames and a camera frame rate of F=60Hz, we had 30Hz, 20Hz and 10Hz frequency bins available. We obtained the demodulated data for two channels, corresponding to 30 Hz (for 647 nm channel) and 20 Hz (for 561 nm channel). Insight3 (a kind gift of Bo Huang, UCSF) was used to localize the fluorescent molecules in each channel of the demodulated frames by performing a simple Gaussian fitting (2D) or elliptical Gaussian fitting (3D) as previously described (4).

Given that the percentage of correct fluorophore assignment was always higher than 96% for fm-DNA-PAINT, a crosstalk correction step was not required. Nevertheless, a simple additional step can be used to further reduce the crosstalk (SI Appendix, **Fig. S2**). In this step, localizations in both color channels were identified if they appeared in the same frame within a distance of 80nm. We computed the sum of intensity values within a 3x3 pixels subROI around the center of each of these localizations in the demodulated data and compared the intensities between both channels. Since the integrated intensity is directly related to the amplitudes of the frequency bins in the frequency domain, we used this information to assign the localization to the correct color channel. This step further reduces the crosstalk to less than 1% in the Cy5 channel and less than 3% in the Cy3 channel (SI Appendix, **Fig. S2**).

**Localization precision calculation:**

We determined the localization precision in two ways. *First*, from the experimental data we

measured the standard deviations of clusters of localizations originated from a single fluorophore (4, 5). To generate traces over several frames of the same fluorophore, a spatial threshold between consecutive frames of 55 nm was set. A minimum track length of 8 frames was set in order to have enough points to properly estimate the localization precision (SI Appendix, **Fig. S3a**). *Second*, we calculated the localization precision by obtaining the Cramér-Rao lower bound (CRLB) of the *x* and *y* position parameters from the Maximum Likelihood Estimation Gaussian 2D fitting of the single molecules, as previously described (6). We used the software provided in reference (6) and followed the suggested procedure. We estimated a $\sigma_{psf}$ of around 1 pixel, so we used a box size of 7x7 pixels ($2x3\sigma_{psf} + 1$) around each localization. We calculated first $\sigma_x$ and $\sigma_y$ and then the x-y localization precision (shown in SI Appendix, **Fig. S3b**) by:

$$\sigma = \sqrt{\sigma_x^2 + \sigma_y^2}$$

For fm-DNA-PAINT, 2 sine-wave modulated lasers were used with a maximum laser power of ~300W/cm$^2$ and an exposure time of 16 ms. For regular DNA-PAINT a continuous illumination with constant laser power of ~300W/cm$^2$ with an exposure time of 100 ms was used. The somewhat lower localization accuracy of fm-DNA-PAINT as compared to regular DNA-PAINT is simply due to the fact that we use modulated excitation, so that fluorophores are excited half of the duration of a single frame, and thus emit roughly half of the photons compared to continuous excitation. Note that given the low laser power excitations used for fm-DNA-PAINT, the SNR could be increased and the subsequent localization precision could be improved, simply by increasing the laser powers.

The localization precision for fm-STORM data was estimated following the first approach since it accounts for the experimental conditions and it is well-accepted in the literature (4, 5).

**Synthetic data:**

We first generated sinewaves for each channel frequency (*f*), depending on camera frame rate (*F*) and frame window size (*m*). The sinewaves were then integrated within the time limits of consecutives frames to obtain an effective integrated intensity per frame (see SI Appendix, **Fig. S5b**). We used this information to generate synthetic data, taking as input a 5x5 pixels subROI of a PSF from one frame of single-color experimental data. Then, 5x5 pixels stacks were generated by multiplying the PSF by the effective integrated intensity per frame over several consecutive frames. In this way, we could simulate the emission of a fluorophore under sinewave modulated illumination. SI Appendix, **Fig. S5c** compares the intensity evolution over time of 2-color synthetic data with that of 2-color fm-DNA-PAINT experimental data, showing excellent agreement between synthetic and experimental data and validating our approach. We followed a similar procedure for generating the 5-color synthetic data (see SI appendix, **Fig. S6**) which is shown in **Fig. 3** of the main text after demodulation. In this case, we used $f_i$=50Hz, 40Hz, 30Hz, 20Hz and 10Hz, *F*=100Hz and *m*=10. The 5 different types of PSFs were spatially mixed, such that spatial overlap could occur. We ranged the spatial distances between the centers of each PSF from 20 pixels (for non-overlapping conditions) to 0 pixels (i.e., full spatial overlap). Note that

this synthetic data has been generated under the assumption of spectrally distinct fluorophores and have minimum overlap in their absorption spectra.

**Semi-synthetic data:**
A 5x5 pixels stack over 6 consecutive frames around the center of a PSF from the fm-DNA-PAINT experimental data was extracted. We performed this procedure for the two different color-fluorophores. In the experimental data, the 647nm laser was modulated at $f$=30Hz for Cy5, and the 561nm laser was modulated at $f$=20Hz for Cy3. Those 5x5 PSFs were replicated 168 times per color, and spatially distributed in order to generate semi-synthetic stacks of images. Several stacks were created, with different relative distances between the centers of the PSFs of both color channels (i.e., $D_{shift}$ in SI Appendix, **Fig. S8a**), ranging from +4 pixels to -4 pixels for spatially overlapping fluorophores and +5 pixels or larger (or -5 pixels or smaller) for the non-overlapping ones. An example of the semi-synthetic data is shown in SI Appendix, **Fig. S7**. In order to generate the background that also fluctuates with the sine-wave modulated lasers illumination, we took a similar 5x5 pixels stack over the same 6 consecutive frames of the experimental data on a background region, i.e., devoid of fluorophores. We then added the background associated to each frame in the corresponding synthetic frame.
The 6-frame semi-synthetic stacks were demodulated to generate 2 demodulated frames, one per channel. Then the centers of the PSFs in those demodulated frames were localized by fitting a 2D Gaussian and the distances from the retrieved localization positions ($x$,$y$) to the real, simulated positions (the pixel where the center of the PSF was positioned) was computed ($D_{relative}$ in SI Appendix, **Fig. S8a**). Plots of $D_{relative}$ as a function of spatial overlap ($D_{shift}$) were generated to estimate the effect of Cy3 spatial overlap on the Cy5 channel (SI Appendix, **Fig. S8b**) and effect of Cy5 spatial overlap in the Cy3 channel (SI Appendix, **Fig. S8c**). Moreover, to estimate the effect of fluorophore brightness on the perturbations to the localization positions for spatially overlapping fluorophores (set to +3pixels), we generated stacks by varying the relative brightness of one color-fluorophore with respect to the other. For this, all the pixels within the 5x5 PSF corresponding to Cy3 (561nm channel) were multiplied by a reduction a factor ranging from 0.5 to 1. The results are plotted in SI Appendix, **Fig. S9**.

**fm-STORM data analysis:**
Background was subtracted using a median filter. Fluorescent molecules were localized in the raw data using Insight3 and performing a simple Gaussian fitting. Localizations were subsequently classified as single-frame or multi-frame localizations. If a fluorophore that appeared in one frame did not move by more than half a pixel (80 nm) in the subsequent frame, it was taken as the same fluorophore and classified as multi-frame. A frame window size was chosen for the demodulation, depending on the desired number of channels and imaging conditions. We used a 4 frame window size for 2-color imaging and a 6 frame window size for 3-color imaging. A 4x4xm voxel region around the centroid (x,y,f)→(x,y,f+m) coordinate of a localization was sliced from the background-suppressed camera data. First, we calculated the mean intensity value of the 16 pixels in the subROI for each raw frame within the frame window, from which we end up with a m-length vector of time-domain data. On these data we performed a one dimensional discrete real-valued Fourier Transform, which yields (m/2) AC components and 1 DC component in the

frequency domain. We used the Python's rfft function from scipy.fftpack (7). Lastly, the absolute values from the FFT for the different frequency bins on the frequency domain were calculated and recorded. Based on the natural logarithm of these values, the localizations were classified into a specific channel. We used the natural logarithms of the demodulated amplitudes rather than the raw values; the distributions of the latter are highly skewed with amplitudes clustered near the origin, while the distributions of the former are more symmetric and can be approximated to first order as rotated asymmetric normals. To perform the channel assignment, decision boundaries were generated by a machine learning algorithm based on a support vector classifier (SVC) (see below Machine learning algorithm for crosstalk correction). The performance of an SVC is typically improved with standard-scaled data that has mean=0 and standard deviation=1, but we find that scaling the amplitudes of our data using only a natural logarithm yields very good results.

**Machine learning algorithm for crosstalk correction:**

Training data sets were acquired using one-color biological samples, which were labeled with the same dyes used for the two-color imaging and imaged in exactly the same way as the two-color samples. The training data was demodulated and the intensities around the localizations corresponding to 4 x 4 pixel subROI were used to define 2D decision boundary regions for those two dyes. The same procedure can be applied for three or more colors. The boundary regions were defined using an SVC. In particular, we used the SVC class contained in the Scikit-learn (8) Python package, which uses libsvm and liblinear libraries (9, 10) for the computations. SVC are well established supervised learning methods used for classification in high dimensional spaces, using training data points in the decision function (called support vectors) and that can use different kernel functions to construct the decision function. Therefore, it can perform multi-class classification on a dataset, taking two inputs: the training datasets and the sample data. SVC implements the one-against-one approach (11) . We used the Radial Basis Function (RBF) as kernel function defined by the following equation:

$$K(x_i, x_j) = e^{-\gamma \cdot \|x_i - x_j\|^2}$$

where $x_i$ and $x_j$ are the support vectors and $\gamma$ defines how large the influence of a single training example is. We used $\gamma$ parameter in "auto" mode. SVC uses training datasets vectors x and an array of class labels y as inputs. The boundary regions are generated by the decision function:

$$sgn\left(\sum_{i=1}^{n} y_i \alpha_i K(x_i, x) + \rho\right)$$

where $\rho$ is the independent term and the $\alpha_i$ are coefficients between 0 and C (see reference S11 for detailed information). C is an input parameter that trades off misclassification against simplicity of the decision boundaries. We used a fixed value of C=1.0. For generating the boundary regions and the fluorophore classification of the multi-color images, we identify and

eliminate data that correspond to localizations which appear in only a single frame in the N-frame demodulation window. These localizations are readily identified by recognizing that a single-frame event in the time domain is effectively a Dirac function, which has a uniform distribution of amplitudes across the frequency domain, and hence will appear along the equal-amplitude y=x line in a two-color measurement and the equivalent functions in higher-dimensional space. Furthermore, these single- frame events typically have low amplitudes relative to multi-frame events, and so appear in a distinct region of the log-log amplitude plot compared to multi-frame events. This undistinguishable population of localizations appeared with a circular shape centered around (6,6) on the 2D single-frame localizations diagram that plots the logarithm of the intensities. We used a rejection radius of 0.8 to reject these localizations. We also eliminate a subset of localizations that appear along the equal-amplitude line with high amplitudes. These localizations appear in both the training data and the experimental data for multiple fluorophores, and so yield no distinct information about the species of molecule underlying that localization. This last step has an additional advantage of preventing the SVC from over-fitting during training. We defined an acceptance ratio parameter that can be changed accordingly from 0 to 1, to achieve a compromise between the percentage of rejected localizations and the final crosstalk between different channels. We used an acceptance ratio of 0.96. The classifier was trained on a randomized sample of 60% of the total training data, with 20% reserved for cross-validation of the SVC and a further 20% used to generate performance scoring metrics.

## SI References:


1. Bálint Š, Verdeny Vilanova I, Sandoval Álvarez Á, Lakadamyali M (2013) Correlative live-cell and superresolution microscopy reveals cargo transport dynamics at microtubule intersections. *Proc Natl Acad Sci*. doi:10.1073/pnas.1219206110.
2. Erdelyi M, et al. (2013) Correcting chromatic offset in multicolor super-resolution localization microscopy. *Opt Express*. doi:10.1364/OE.21.010978.
3. Tokunaga M, Imamoto N, Sakata-Sogawa K (2008) Highly inclined thin illumination enables clear single-molecule imaging in cells. *Nat Methods*. doi:10.1038/nmeth1171.
4. Huang B, Wang W, Bates M, Zhuang X (2008) Three-dimensional super-resolution imaging by stochastic optical reconstruction microscopy. *Science (80- )*. doi:10.1126/science.1153529.
5. Rust MJ, Bates M, Zhuang X (2006) Sub-diffraction-limit imaging by stochastic optical reconstruction microscopy (STORM). *Nat Methods*. doi:10.1038/nmeth929.
6. Smith CS, Joseph N, Rieger B, Lidke KA (2010) Fast, single-molecule localization that achieves theoretically minimum uncertainty. *Nat Methods*. doi:10.1038/nmeth.1449.
7. Oliphant TE (2007) SciPy: Open source scientific tools for Python. *Comput Sci Eng*. doi:10.1109/MCSE.2007.58.
8. Pedregosa F, et al. (2012) Scikit-learn: Machine Learning in Python. *J Mach Learn Res*. doi:10.1007/s13398-014-0173-7.2.
9. Chang C, Lin C (2013) LIBSVM : A Library for Support Vector Machines. *ACM Trans Intell*

*Syst Technol*. doi:10.1145/1961189.1961199.
10. Fan R-E, Chang K-W, Hsieh C-J, Wang X-R, Lin C-J (2008) LIBLINEAR: A Library for Large Linear Classification. *J Mach Learn Res*. doi:10.1038/oby.2011.351.
11. Knerr S, Personnaz L, Dreyfus G (1990) Single-layer learning revisited: a stepwise procedure for building and training a neural network. *Neurocomputing* doi:10.1007/978-3-642-76153-9_5.

## Supplementary Figures

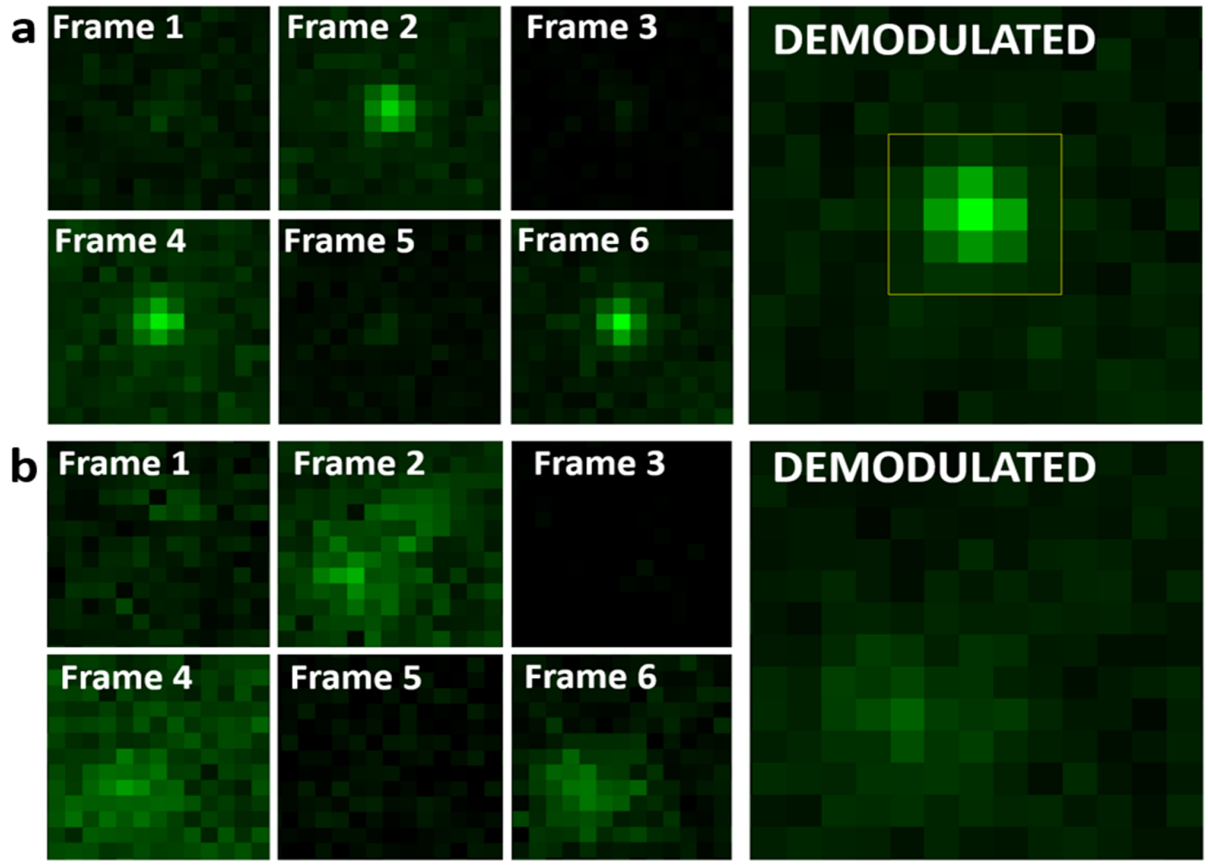


**Figure S1: Effect of diffusing molecules on fm-DNA-PAINT:** (**a**) Individual frames corresponding to a bound molecule in fm-DNA-PAINT (left) and the corresponding point spread function (PSF) of the molecule after demodulation (right). The PSF is bright enough to be localized by the localization algorithm (yellow square). (**b**) Individual frames corresponding to a diffusing molecule in fm- DNA-PAINT (left) and the corresponding point spread function (PSF) of the molecule after demodulation (right). The PSF is too dim to be localized by the localization algorithm.

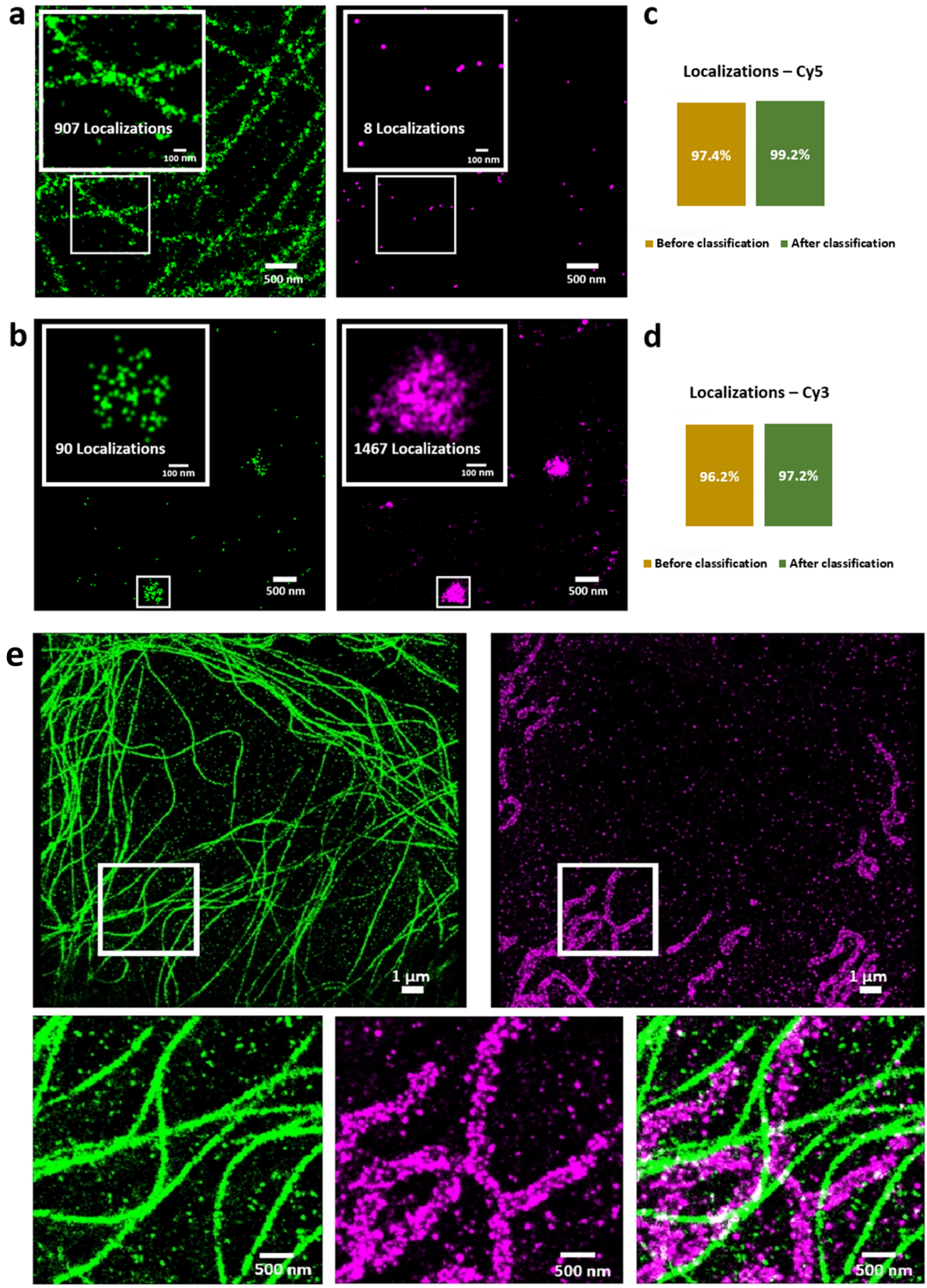


**Figure S2: Color cross-talk quantification and correction in fm-DNA-PAINT. (a-b)**

Microtubules (green) (**a**) and lysosomes (magenta) (**b**) labeled with Cy5-equivalent and Cy3-equivalent dyes alone, respectively and imaged in two colors using fm-DNA-PAINT. Images show the results before crosstalk correction. The green localizations correspond to the Cy5 channel and the magenta localizations correspond to the Cy3 channel. Localizations in a region of interest around the imaged structure were quantified in the two channels (white boxes and insets). (**c-d**) Percentage of localizations belonging to the Cy5 (**c**) or Cy3 (**d**) channels before color cross-talk correction (yellow bars) and after color cross-talk correction (green bars). (**e**) Two-color super-resolution image of microtubules and mitochondria imaged using fm-DNA-PAINT, after crosstalk correction (same image shown in main Fig. 1c with the display split into two channels). Upper left panel shows microtubule channel only and upper right panel shows mitochondria channel only. Lower panel shows a zoom region (highlighted with a white box) of the microtubules, mitochondria and the overlay.

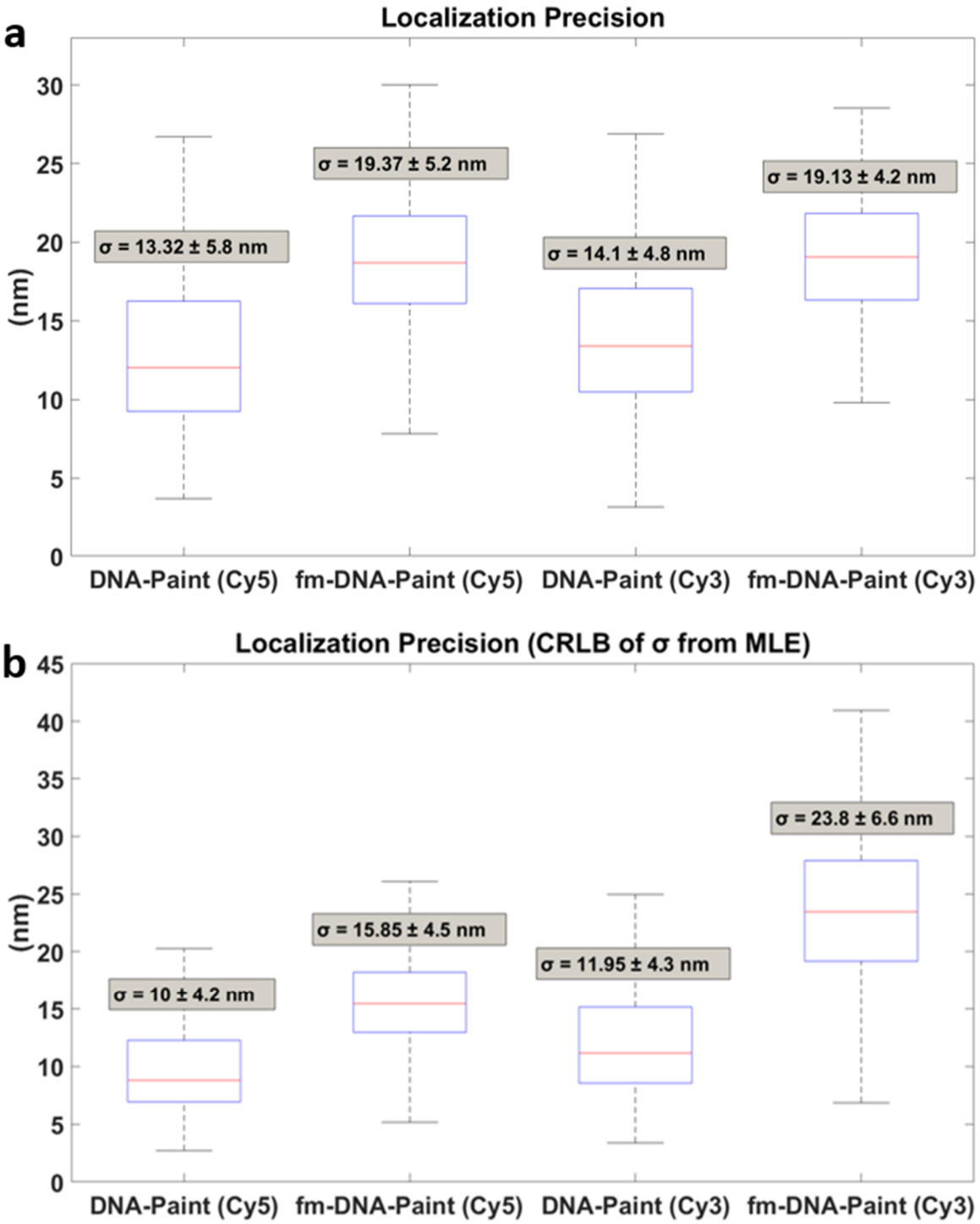


**Figure S3: Localization precision comparison between conventional and fm-DNA-PAINT.** **(a)** Localization precision calculated from the standard deviation of the localizations of the same fluorophore in multiple frames (minimum of 8) and compared between conventional DNA-PAINT with 100 ms exposure time and fm-DNA-PAINT with 16 ms exposure time and 6 frame window size, for Cy5 and Cy3 fluorophores. **(b)** Comparison of the localization precision obtained from

Cramer-Rao Lower Bound of the MLE Gaussian fitting. For both (a) and (b) the mean σ ± the standard deviation are indicated in the box plots. Laser excitation powers were identical for conventional DNA-PAINT and fm-DNA-PAINT, i.e., 300W/cm$^2$. The box indicates the 25$^{th}$ ($q_1$) and 75$^{th}$ ($q_3$) percentiles. The whiskers extend to the most extreme data value that was not considered an outlier. Outliers are values bigger than $[q_3 + 1.5\cdot(q_3 - q_1)]$ or smaller than $[q_1 - 1.5\cdot(q_3 - q_1)]$. Around 99.3% (or ±2.7σ) of the data lies within these whiskers values.

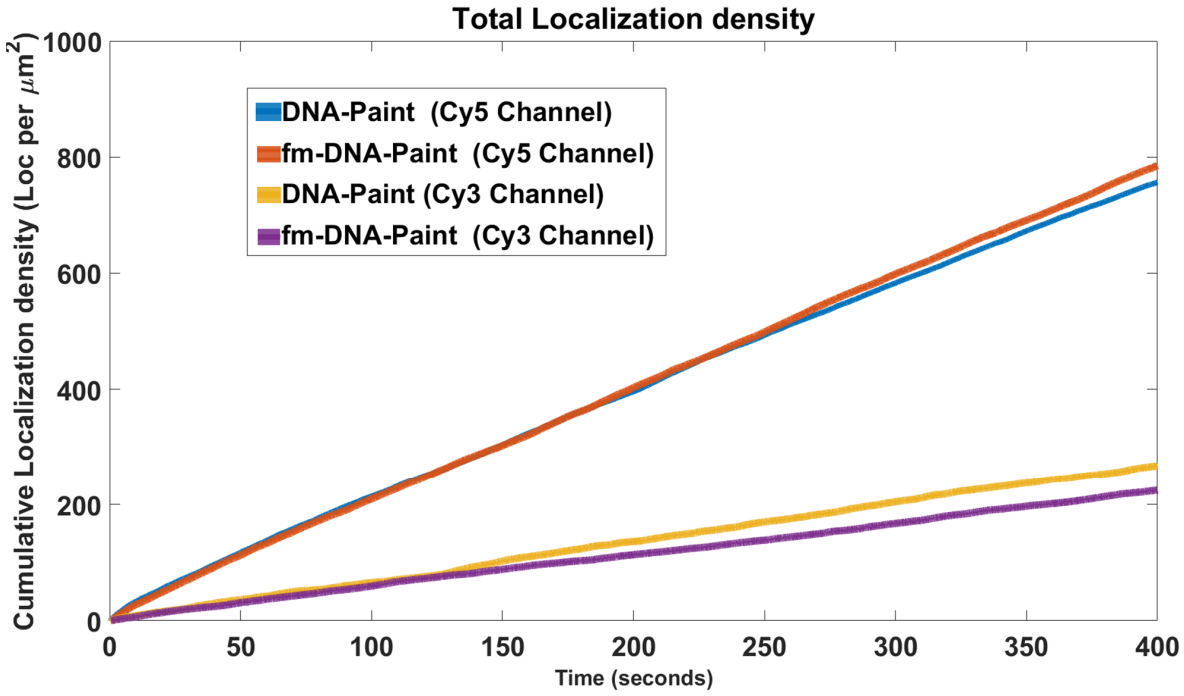


**Figure S4: Cumulative localization density as a function of time.** Number of localizations per frame in both DNA-PAINT and fm-DNA-PAINT grow linearly with the number of frames, since in both cases there is inexhaustible amount of fluorophores. No differences are measured in terms of the total localization density as a function of time between conventional and fm-DNA-PAINT. The difference in the slopes between the Cy5 and Cy3 channels is only due to differences in the concentrations of the fluorophores used for the experiments, being higher in the Cy5, 647 nm channel than in the Cy3, 561 nm channel.

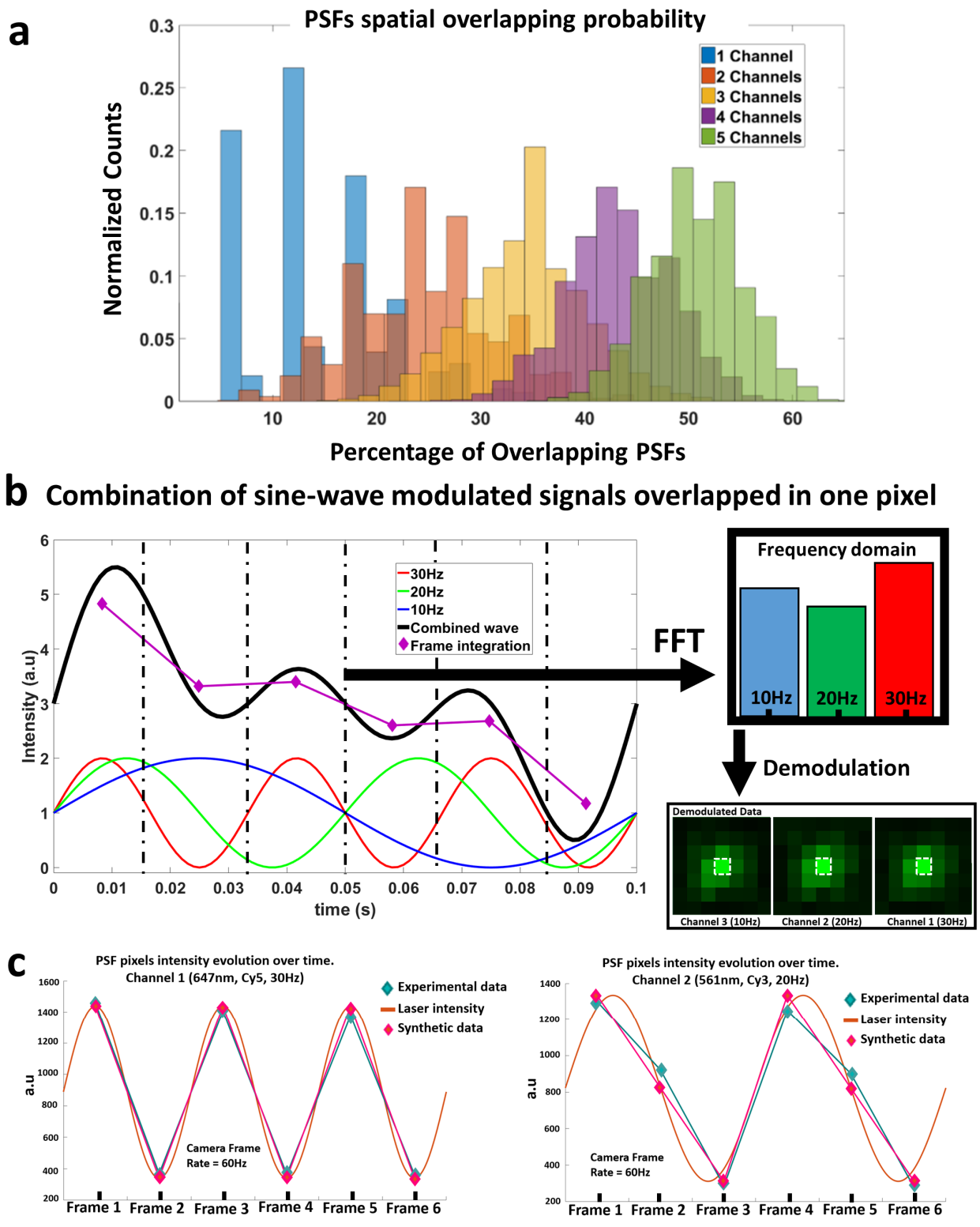


**Figure S5: Effect of the spatial overlap between spectrally distinct fluorophores (Cy5-equivalent and Cy3-equivalente) in fm-DNA-PAINT. (a)** Histogram showing the probability of spatial overlap between randomly distributed fluorophores with a PSF of 5x5 pixels

(800x800nm) and a constant PSF density per frame of 0.1 localization/$\mu m^2$. The probability of spatial overlap is shown for one-to-five color channels. **(b)** Example of one pixel intensity evolution in time domain when three spectrally distinct fluorophores overlap spatially. The three fluorophores are modulated with excitation laser frequencies of 10 Hz, 20 Hz and 30 Hz. The red, green and blue lines correspond to the sinewave modulation of the three lasers. The black line is the combination of these individual sinewaves. The magenta line is the integration of the combined sinewave over each frame (16 ms in this case), which is proportional to the pixel intensity signal, due to the response of the three overlapping fluorophores to the three sinewave modulations. Note that a 6 frame window size ($m$=6) is used, and thus 6 pixel values are calculated. In the frequency domain the pixel can be properly demodulated into the three different color channels. The white square in the demodulated data shows the demodulated pixel in the three corresponding channels. The intensity of the pixel on the reconstructed (demodulated) image is proportional to the amplitude in that particular frequency in the frequency domain. **(c)** The response of fluorophores to sinewave modulated laser excitation obtained from experimental data. The orange line shows the modulated sinewave excitation. The blue diamonds are the measured intensity of the fluorophore over 6 frames in response to the sine wave excitation. The magenta diamonds are the generated intensity of the fluorophore in the synthetic data over 6 frames. The blue and magenta lines are guides to the eye.

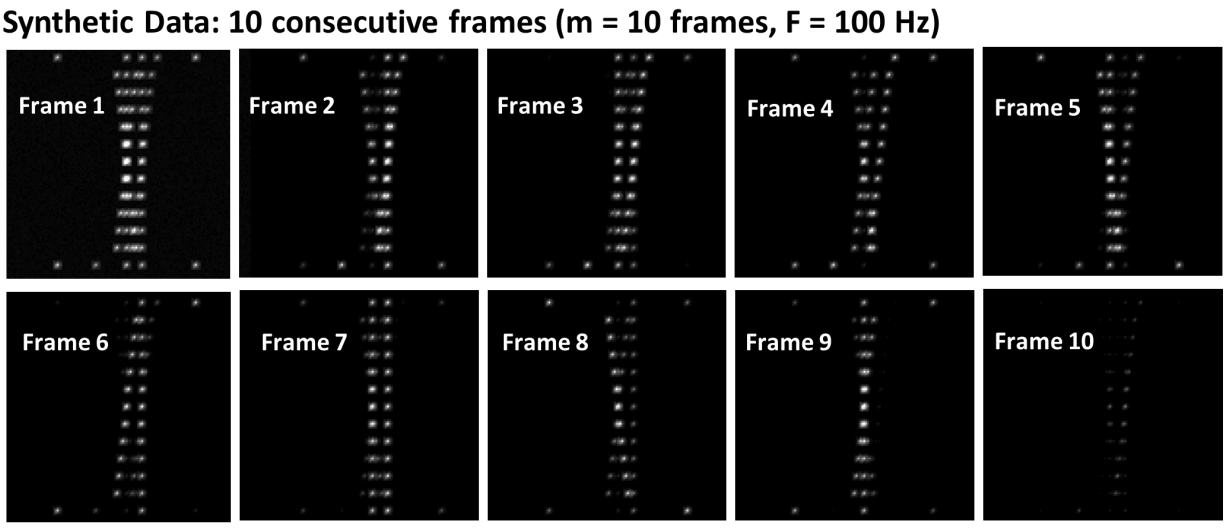


**Figure S6: Synthetic raw data for 5-color fm-DNA-PAINT.** 5-color synthetic image generated with camera frame rate $F$=100Hz and $f_i$ of 50Hz, 40Hz, 30Hz, 20Hz and 10Hz, assuming that the fluorophores have minimal spectral overlap (similar to the 2-color experimental data with Cy5 and Cy3). Ten consecutive frames from the synthetic raw data are shown. The brightness of the pixels in each frame reflects the integrated intensity of the modulated excitation. The corresponding demodulated frames for each channel are shown in **Fig. 3** on the main text.

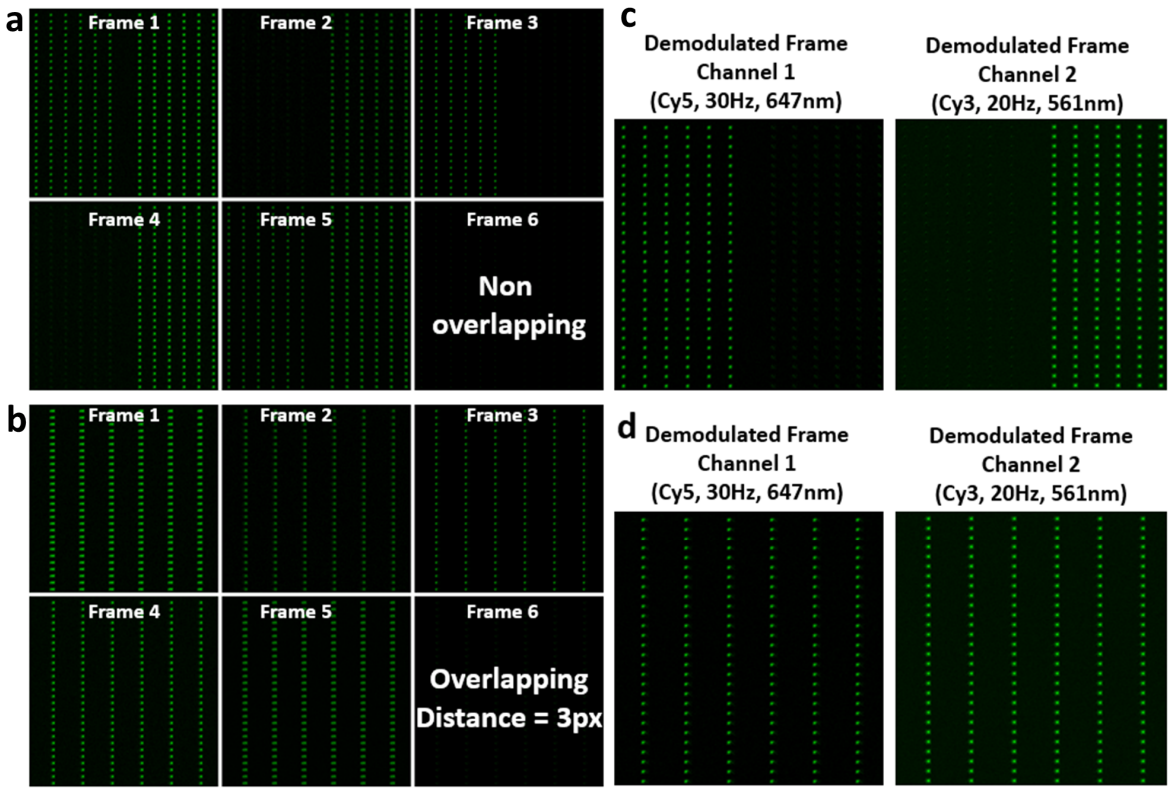


**Figure S7: Semi-synthetic data to assess the effect of spatial overlap on the localization precision of fm-DNA-PAINT. (a)** 6 consecutive frames of the semi-synthetic dataset in the absence of spatial overlap between the two spectrally distinct fluorophores (Cy5-equivalent, left 6 stripes and Cy3-equivalent, right 6 stripes) illuminated with lasers at different modulation frequencies (30Hz and 20Hz respectively). The camera frame rate is $F$=60Hz. 168 PSFs per channel were generated. The difference in brightness in the frames reflects the integrated excitation intensity for the different modulated lasers. **(b)** Similar as (a) but with an overlapping of 3 pixels between the two color channels. **(c)** Corresponding demodulated frame of the image stack in **a** for both channels. **(d)** Corresponding demodulated frame of the image stack with spatially overlapping fluorophores in **b** for both channels.

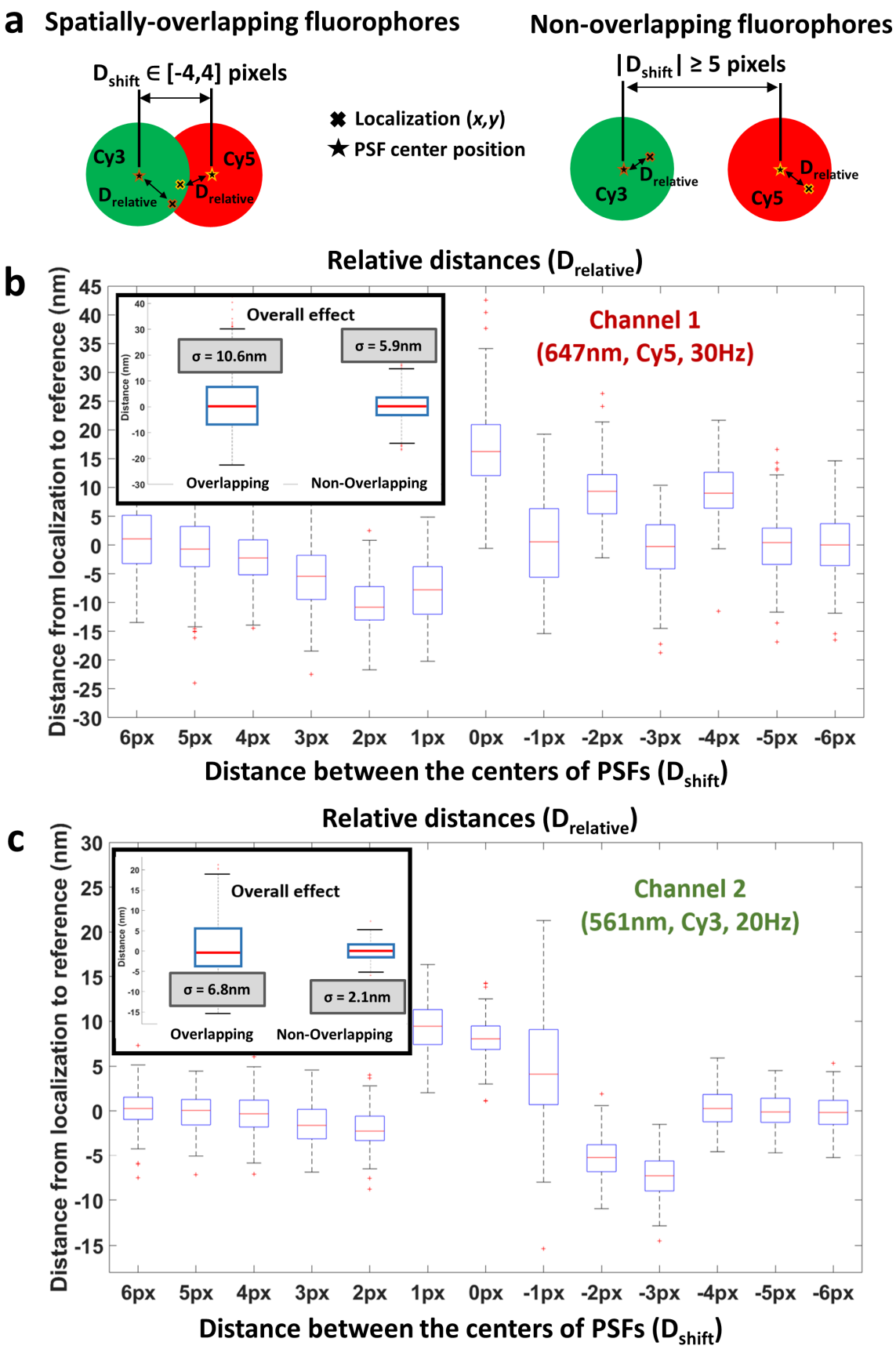
a
Spatially-overlapping fluorophores
Non-overlapping fluorophores
D_shift ∈ [-4,4] pixels
|D_shift| ≥ 5 pixels
Localization (x,y)
PSF center position
Cy3
Cy5
D_relative
b
Relative distances (D_relative)
Channel 1
(647nm, Cy5, 30Hz)
Overall effect
σ = 10.6nm
σ = 5.9nm
Overlapping
Non-Overlapping
Distance from localization to reference (nm)
Distance between the centers of PSFs (D_shift)
6px
5px
4px
3px
2px
1px
0px
-1px
-2px
-3px
-4px
-5px
-6px
c
Relative distances (D_relative)
Channel 2
(561nm, Cy3, 20Hz)
Overall effect
σ = 6.8nm
σ = 2.1nm
Overlapping
Non-Overlapping
Distance from localization to reference (nm)
Distance between the centers of PSFs (D_shift)

**Figure S8: Effect of the spatial overlap between spectrally distinct fluorophores (Cy5-equivalent and Cy3-equivalente) on localization accuracy in fm-DNA-PAINT. (a)** Cartoon showing the method used for estimating the perturbation on the localization position produced by the spatial overlap of spectrally distinct fluorophores, for overlapping (left) and non-overlapping (right) conditions. The green and red circles denote the two different fluorophores, with their real center positions marked by the star symbol. $D_{shift}$ corresponds to the spatial shift between the different colored PSFs in the semi-synthetic data. After demodulation, the *x,y* positions are determined (cross symbols) and $D_{relative}$ (distance between the localized positions and the real positions) is measured. Thus, $D_{relative}$ is a measure of the spatial overlap influence that one color-fluorophore has on the localization position of the other color-fluorophore after demodulation. **(b)** Effect of Cy3 spatial overlap on the localization position of the Cy5 channel, for different degrees of spatial overlap, i.e., $D_{shift}$. The inset shows the combined distribution for all overlapping pixels and all non-overlapping pixels. **(c)** Effect of Cy5 spatial overlap on the localization position of the Cy3 channel, for different degrees of spatial overlap, i.e., $D_{shift}$. The inset shows the combined distribution for all overlapping pixels and all non-overlapping pixels. Although in principle one would expect $D_{relative}$ to be zero in the complete absence of spatial overlap, $D_{relative}$ is also influenced by the difference in brightness and background of the fluorophores. This is because our generated semi-synthetic data uses experimental input data including background. Therefore slight variations in the fluorophore brightness and/or background will lead to small deviations in the demodulated localization positions. For the generated *in-silico* data, this effective localization error is around 5.9 nm for Cy5 and 2.1 nm for Cy3. Notice that the influence of spatial overlap in the localization position of the fluorophores is larger for Cy3 than for Cy5, i.e., a factor of 3 for the influence of Cy5 in the position of Cy3 and only a factor of 1.8 for the influence of Cy3 in the position of Cy5. This result is entirely consistent with the fact that Cy5 absorbs about 10% of the Cy3 excitation wavelength (561nm) and thus it would induce a larger perturbation on the Cy3 channel. In (b) and (c) the box indicates the 25$^{th}$ ($q_1$) and 75$^{th}$ ($q_3$) percentiles. The whiskers extend to the most extreme data value that was not considered an outlier. Outliers are values bigger than $[q_3 + 1.5 \cdot (q_3 - q_1)]$ or smaller than $[q_1 - 1.5 \cdot (q_3 - q_1)]$.

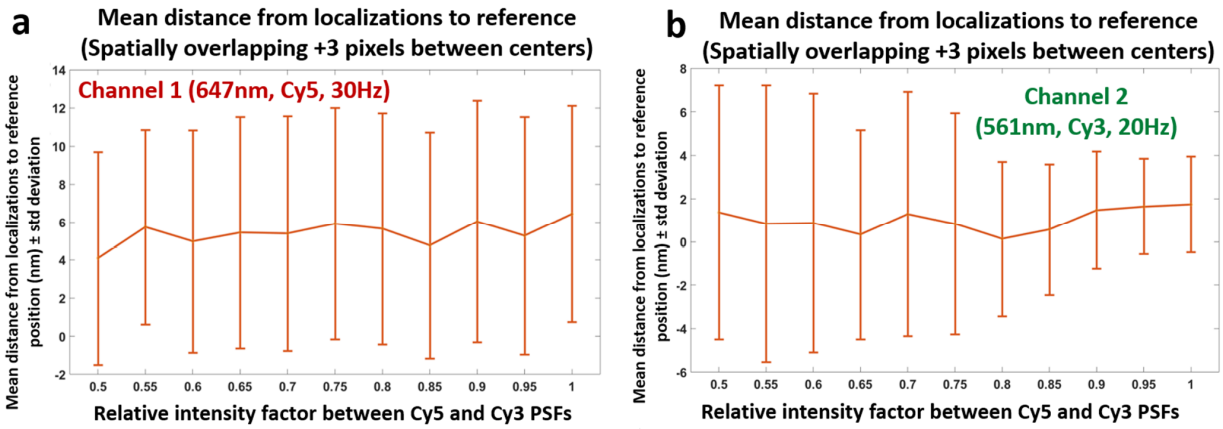


**Figure S9: (a)** and **(b)** Effect of the relative signal between fluorophores on localization accuracy in the presence of spatial overlap. In this case, a constant relative distance of +3 pixels between the centers of the PSFs was set, such that there is spatial overlap. The relative signal between the PSFs was set by generating semi-synthetic data, in which the Cy5 intensity was kept constant and all pixels of Cy3 PSF in the 6 consecutive frames were multiplied by a relative intensity factor (ranging from 1 to 0.5). The vertical bars are the standard deviation.

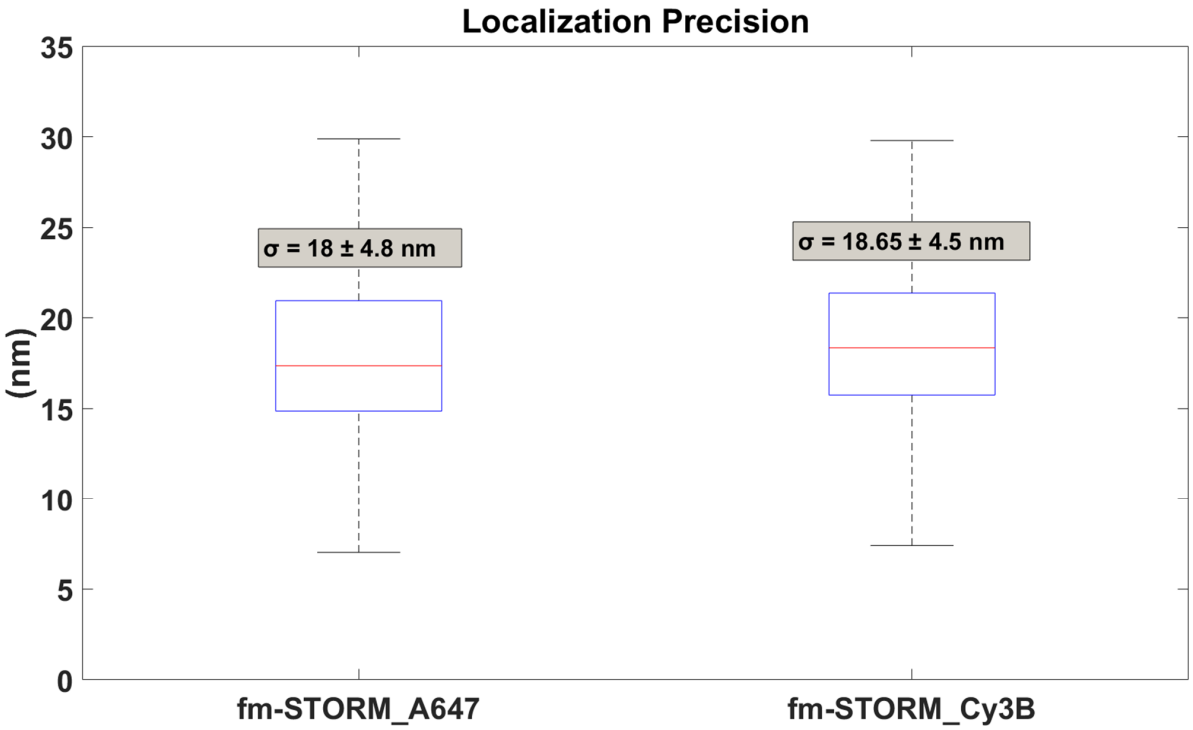


**Figure S10: Localization precision in fm-STORM for A647 and Cy3B fluorophores.** Box plot showing the experimental localization precisions obtained for 1-Color fm-STORM, for both channels, corresponding to A647 and Cy3B. The localization precisions have been calculated from the training data sets with camera frame rate $F$=90Hz, 647nm laser sinewave modulated at $f_1$=45Hz and the 561nm laser modulated at $f_2$=22.5Hz. The localization precisions have been determined by obtaining the standard deviation of the localizations over multiple consecutive frames of the same fluorophore. The box indicates the 25$^{th}$ ($q_1$) and 75$^{th}$ ($q_3$) percentiles. The whiskers extend to the most extreme data value that was not considered an outlier. Outliers are values bigger than $[q_3 + 1.5\cdot(q_3 - q_1)]$ or smaller than $[q_1 - 1.5\cdot(q_3 - q_1)]$. Around 99.3% (or ±2.7σ) of the data lies within these whiskers values.

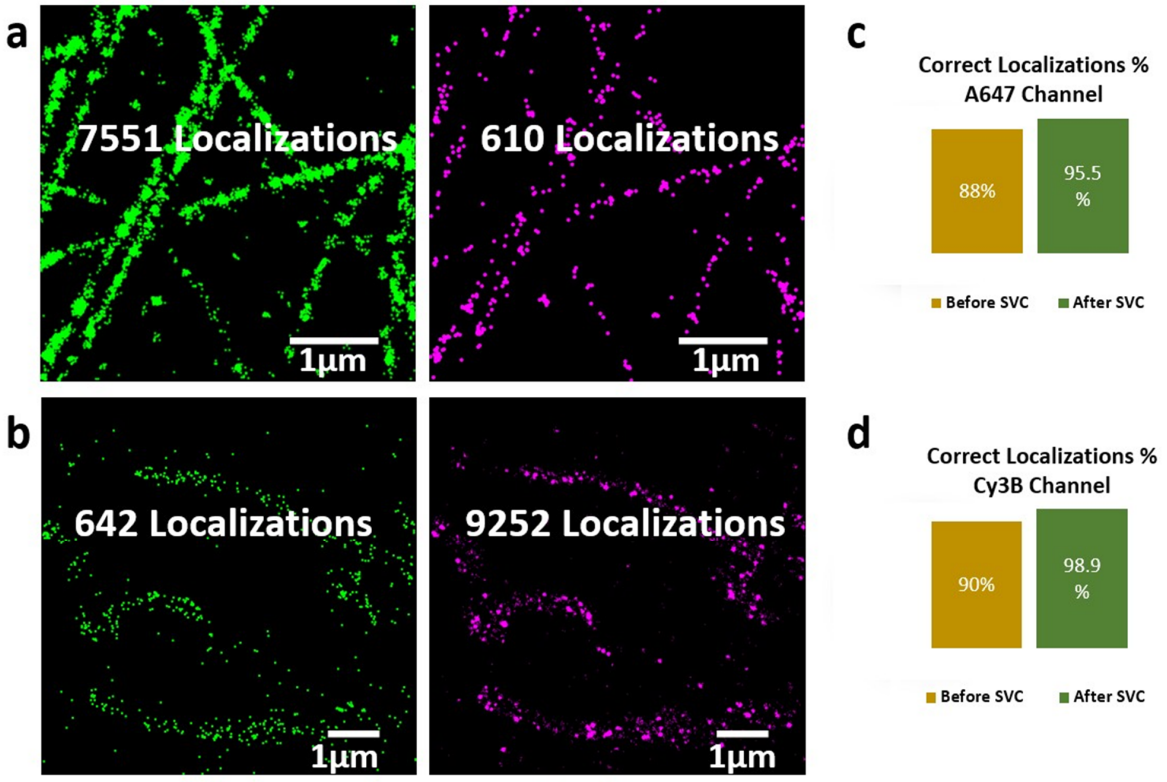


**Figure S11: Color cross-talk quantification in fm-STORM.** (**a, b**) Microtubules (green) and mitochondria (magenta) labeled with AlexaFluor647 (AF647) alone and Cy3B alone, respectively and imaged in two colors using fm-STORM. Images show the two channels before cross-talk correction. The green localizations correspond to the AF647 channel and the magenta localizations correspond to the Cy3B channel. Localizations in the displayed region of interest were quantified in the two channels. (**c, d**) Percentage of localizations belonging to the AF647 (**c**) or Cy3B (**d**) channels before color cross-talk correction (yellow bars) and after color cross-talk correction (green bars) using the machine learning algorithm.

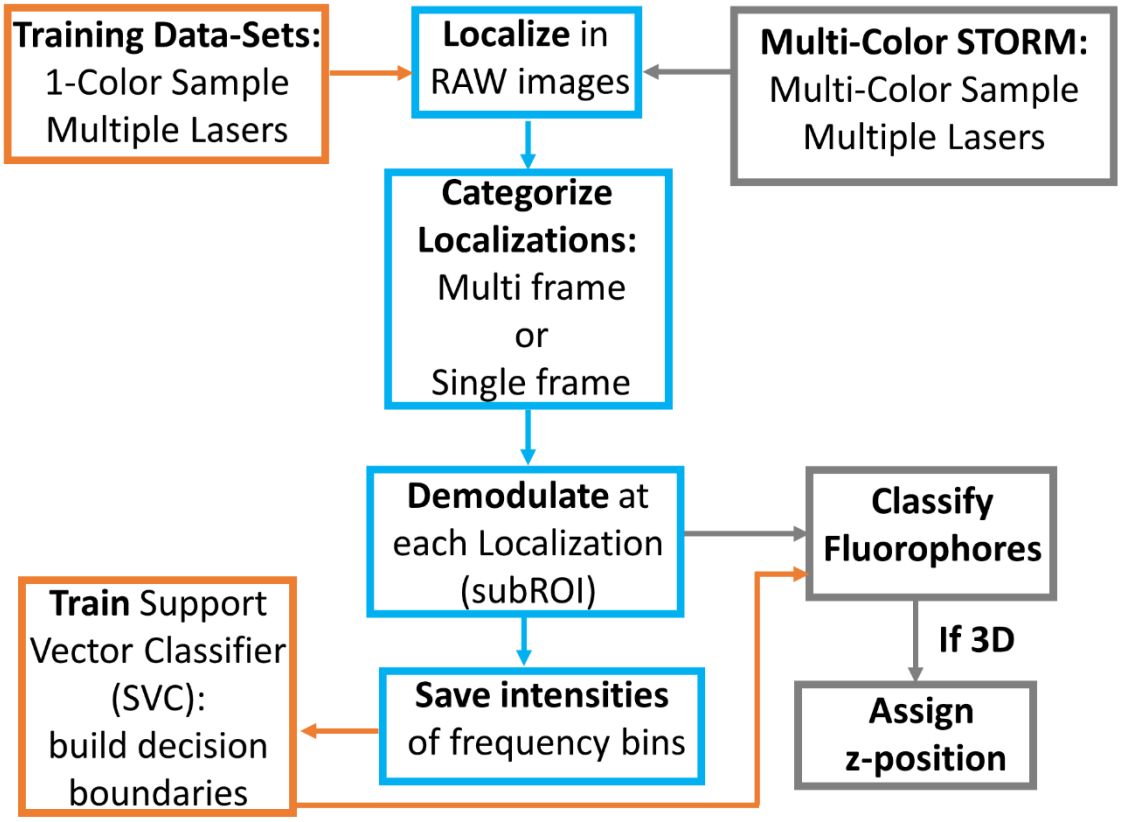


**Figure S12: Workflow of the machine learning algorithm for fluorophore classification in fm-STORM.** The algorithm requires training data sets for each fluorophore and imaging condition, in order to build the decision boundary regions for fluorophore classification. Localizations that appear in only a single frame and those that appear in multiple frames are categorized in order to be processed separately.

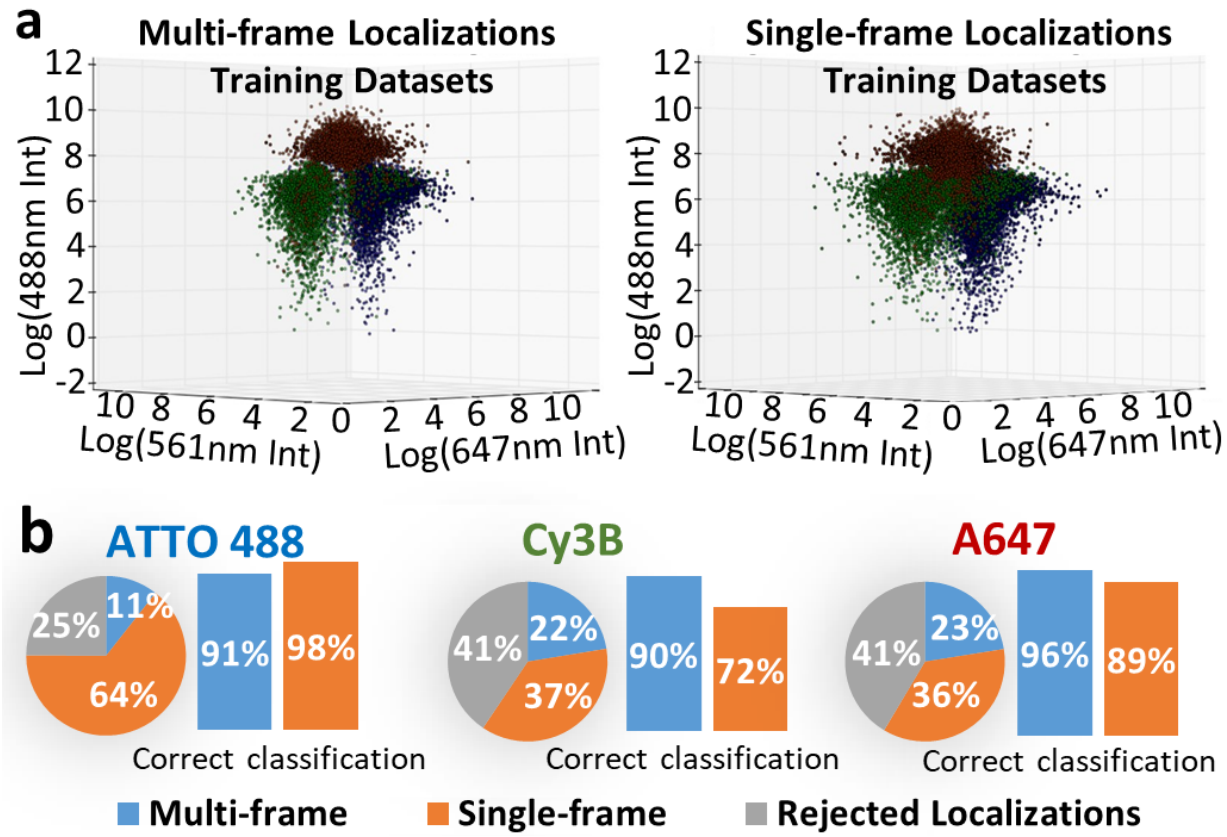


**Figure S13: Training data for cross-talk correction of three color fm-STORM. (a)** Multi- and single- frame localizations obtained from a training dataset using ATTO488, Cy3B and AF647 fluorophores, showing the color-separation in the three channels. **(b)** Percentage of single-frame, multi-frame and rejected localizations for the three fluorophores (pie charts) and the correctly classified single- and multi- frame localizations for three fluorophores (bar charts) calculated from a sub-set of localizations used for the training data

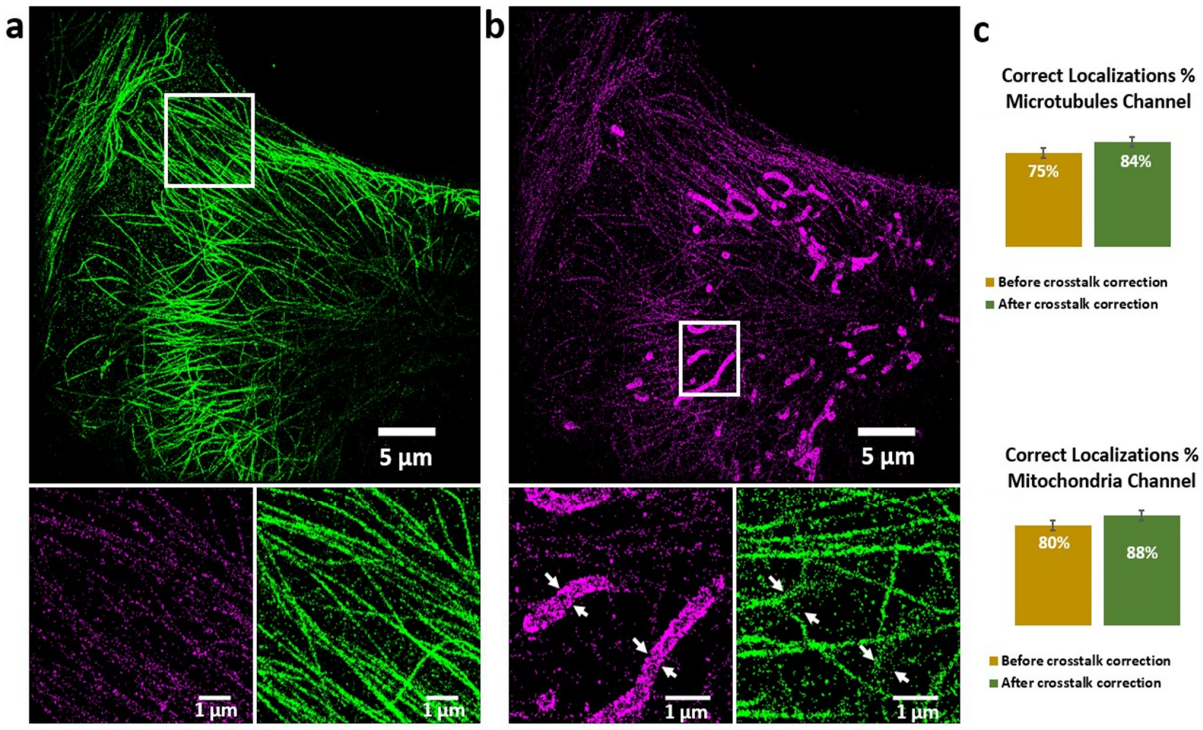


**Figure S14: Two-color STORM image of microtubules and mitochondria imaged using the activator/reporter approach.** Microtubules and mitochondria were labeled with AF405/AF647 and Cy3/AF647 activator-reporter pairs, respectively. Images are shown after standard cross-talk correction. **(a)** Microtubule channel (green) and a zoom-in of the white boxed region where there are microtubules only, displaying both channels (green and magenta). **(b)** Mitochondria channel (magenta) and zoom in of the white-boxed region where mitochondria can be identified (white arrows), displaying both channels (green and magenta). **(c)** Percentage of correct localizations assigned to each channel. Since the two structures are clearly defined and separated, the cross-talk calculation can be performed by counting the number of localizations from the two channels in regions where only one structure is present (i.e. mitochondria-only or microtubules-only regions). Yellow bars shows the values before cross-talk correction and green bars after cross-talk correction using statistical approaches.

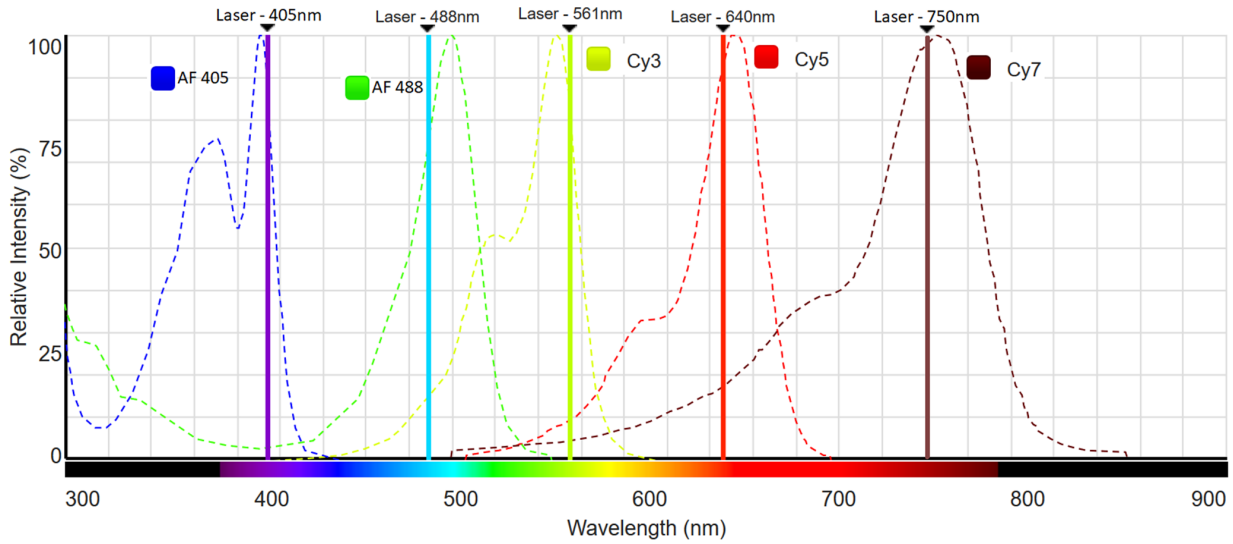


**Figure S15: Absorption spectra of 5 different standard fluorophores for implementation in fm-DNA-PAINT.** Example of 5 different fluorophores with relatively little spectral overlap in their absorption spectra. The suitable lasers for differential excitation of each of the fluorophores is included in the figure. Notice that there is negligible overlap between AF405, AF488, Cy3 and Cy5, and thus, in principle fm-DNA-PAINT of four colors with minimal color crosstalk and in the presence of spatially overlapping fluorophores should be easily obtainable. A somewhat larger spectral overlap exists between Cy5 and Cy7, so that excitation of Cy5 by the 640nm laser line would also marginally excite Cy7, leading to an additional amplitude of Cy7 in the frequency bin of the Cy5 channel. (Adapted from The Spectra Viewer, www.thermofisher.com)